Chapter 2

Pyroelectric Infrared Sensor Module

In Chapter 2 we will discuss essential components used in our systems including pyroelectric sensors, Fesnel lens arrays, micro-controllers, and RF transceiver modules.

2.1 Pyroelectric Sensors

Sensors that measure radiation by means of a change in temperature of an absorbing material are called thermal sensors. One of the most common thermal sensors used in the infrared (IR) applications is the pyroelectric sensor that converts incident thermal radiation into an electrical signal. Pyroelectric materials are those that develop an electric charge in response to a temperature change. The charge that is developed is directly proportional to the change in the temperature. This conversion takes place in two steps; first, the incident thermal radiation results in slight heating of the pyroelectric material. This heating changes the electrical properties of the material, which are capacitive in nature. Second, because charge is conserved, the change in capacitance causes a corresponding change in the signal voltage seen across the sensor's load resistance.

The pyroelectric infrared sensors are utilized for a variety of commercial, industrial and military applications. They can be used over a wide range of temperatures without any temperature controlling mechanism, and the noise limited operation can easily be achieved with relatively simple circuits. There is no need for special power supplies and detector signal processing. In addition, these sensors are cost effective since they are manufactured from generally available single crystal materials and can also very easily be made into many detector configurations and sizes to suit different applications.

2.1.1 Types of Pyroelectric Sensors

Single and dual element sensors are the two types of commercially available detectors. A single element detector consists of a single element that is exposed to the incoming radiation. This configuration is very sensitive to changes in ambient temperature and mechanical vibrations. Temperature compensation is implemented by connecting another sensing element to the body. The ambient effects will be canceled out since both the elements are exposed to the same environmental conditions. Single element detectors perform well in applications where the detector looks at a narrow field of view with a background that changes temperature much slower than the response of the system.

In a dual element detector, as the name suggests, there are two active elements exposed to the incoming radiation. The two elements are placed at a small distance apart so that each has a slightly different field of view. These elements are connected in series opposition, thus providing thermal compensation. Only a differential output is obtained, that is, a dual element detector's output voltage is the difference between the voltages obtained from each of the elements of the detector. Thus, these sensors have the inherent advantage that the impact of environmental temperature fluctuation can be neutralized. It is important to note that the polarity of the signal obtained depends on the orientation of the detector. Hence, direction could be inferred based on the signal obtained knowing how the detector is oriented. Dual element detectors are therefore widely used in motion detection applications since they not only isolate the motion from the ambient, but they also have the capability of indication the direction of motion.

2.1.2 Sensor Characterization

We use a pyroelectric detector PIR325 with two sensing elements obtained from Glolab

Corporation [1]. Using the experimental setup shown in Fig. 2.1, we first measured the step response of the sensor. An incandescent bulb was used as the heat source with an occluding shutter to simulate the sudden change in heat flux incident on the pyroelectric detector. We blocked one of the dual elements to model the step response for a single element. A measured step response of the system is shown as the dashed line in Fig. 2.2. The solid line is the step response of a 4th order transfer function as [2]

$$H(s) = \frac{U(s)}{\Phi(s)} = k_g \left(\frac{s^2 + 2\zeta_t \omega_t s}{s^2 + 2\zeta_t \omega_t s + \omega_t^2} - \frac{s^2 + 2\zeta_e \omega_e s}{s^2 + 2\zeta_e \omega_e s + \omega_e^2} \right), \qquad (2\text{-}1)$$

where $U(s)$ is the amplified voltage signal, $\Phi(s)$ is the thermal flux; the transfer gain k_g =0.26 V/J, the electronic circuit damping ratio ζ_e =0.7, the electronic circuit natural frequency ω_e =2 Hz, the thermal damping ratio ζ_t =0.7, and the thermal natural frequency ω_t =0.6 Hz.

We can see that our detector system is a bandpass system with frequency limits between 0.6 Hz and 2 Hz. A moving human target, with angular velocities between 0.9 rad/s and 3.1 rad/s, would produce signals within this bandwidth, if the sensor has a $\pi/2$ field of view (FOV).

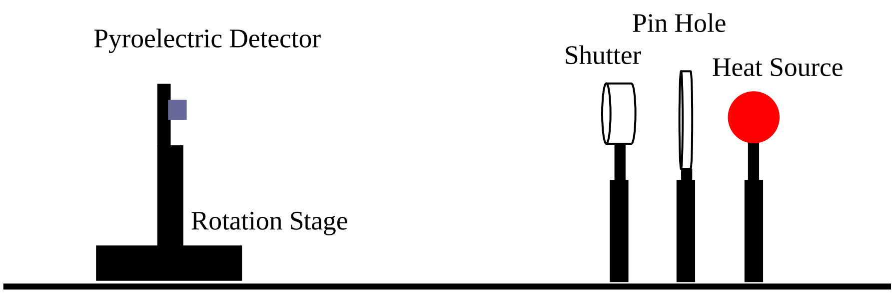

Fig. 2.1 Experimental setup for sensor characterization

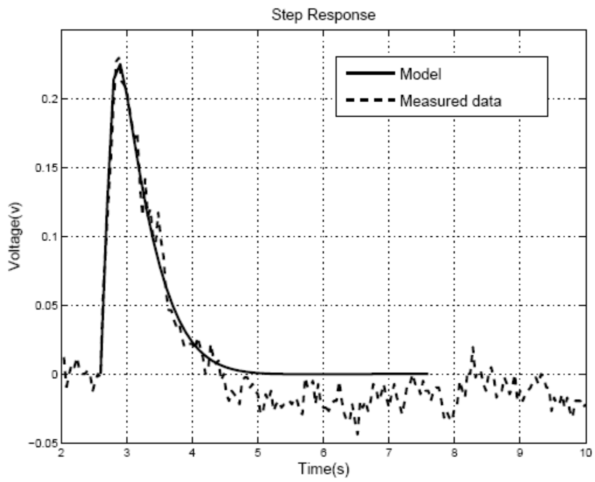

Fig. 2.2 Step response of the pyroelectric sensor.

The next parameter that we characterize is the angular response since we would like to determine the FOV of the detector in order to modulate its visibility for the application desired. The angular response of a detector with dual element was determined using the same setup that was described earlier (Fig. 2.1). Here, the source was kept fixed and the detector was rotated over different angles and the step response was determined at each angle. The response obtained at each of the angles was normalized and plotted as shown in Fig. 2.3. This polar plot was made at between -90^o~90^o and indicates the FOV for a dual element pyroelectric detector. As was expected, the response from the dual element detector resembles two individual single element sensors which are offset by the spatial separation between each of the detectors. It is to be noted that, the response at 0 deg (along the detector axis) is minimum. This is due to the fact that the two elements are connected in series opposition and the signal obtained on each of the detectors from the common area of overlap of the FOV's canceled each other and a minimum is obtained. A significant response is obtained from the regions where there is no overlap of the visibility.

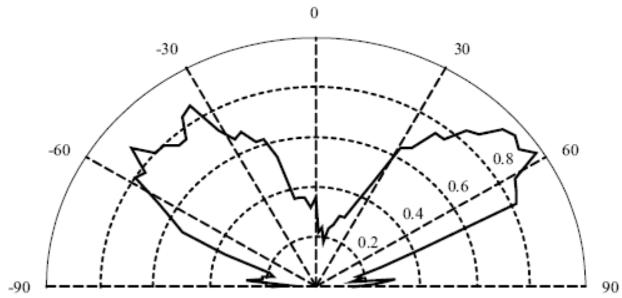

Fig. 2.3 Polar plot of visibility of dual element pyroelectric detector.

The response of the sensor with respect to distance was also determined by using a soldering iron heat source. A chopper is placed in front of the iron to obtain a recognizable sinusoidal signal pattern. By setting the sensor at different distances, we plotted the falloff of the magnitude of the response versus distance in Fig. 2.4. It corresponds to the expected $1/r^2$ dependence.

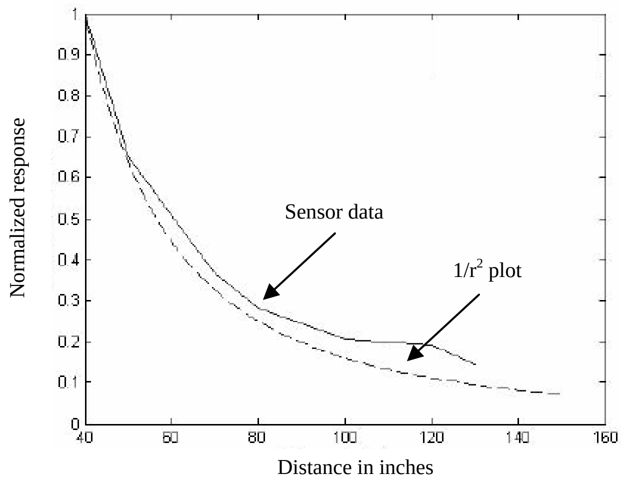

Fig. 2.4 Response of the dual element pyroelectric detector with distance.

2.2 Power Coupled to Detector

The heat flux that is radiated from the body spreads out isotropically. The amount of power that is actually coupled to the detector depends on the collection area of the detector. This power, ϕ_d, that is available at the detector is given by

$$\phi_d = \frac{\psi \times A_{ca}}{r^2} \quad , \tag{2-2}$$

where ψ is the power radiated by the human source as calculated in section 1.3 using Eq. 1.1, A_{ca} is the collection area of the detector and 'r' is the distance of the source from the detector system. Therefore, substituting Eq. 1.2 into Eq. 2.2, we obtain the power that is available at the detector as

$$\phi_d = \frac{A\varepsilon\sigma(T_h^4 - T_c^4)A_{ca}}{r^2} \quad . \tag{2-3}$$

This equation describes the fraction of the total power emitted by the source that actually falls on the detector. As mentioned earlier, the power that actually is available at the detector depends on the energy collection area. If no optics were to be used, this would be the area of the elements of the detector itself. This area is relatively small and hence only a small fraction of the available power would actually be sensed by the detector. As calculated above, the power radiated by the human body is about 100*W*. Substituting the value of the area of the detector in the term A_{ca} as $2mm^2$ and the distance of the source and the detector to be about 2*m*, we get the power that is available at the detector to be about $50\mu W$. This is considering the entire body as the source. However, if smaller sources are considered, say the hand or the fingers, this power will scale down with the area of the emitting surface. If we consider the finger (area$\approx$14cm^2), for example, the power available at the detector is only about 35*nW*. As the distance increases, the amount of power falls off very rapidly. Hence, there is need for some optics in order to increase the collection efficiency.

2.3 Fresnel Lens Arrays

Since the detector elements have a small area, the amount of power collected is a very small fraction of the incident power. To overcome this drawback, we use a Fresnel lens to improve both the collection efficiency and spatial resolution. Fresnel lenses are very good energy collectors and are being used extensively for various applications- magnifying lenses, projectors, car head lights, etc [3, 4]. They can be molded out of inexpensive plastics with desired transmission characteristics (for the required wavelength range) making the system thin, light weight and inexpensive. Furthermore, lens arrays are easily built by stacking them in different orientations to suit each application. Fresnel lens arrays and pyroelectric detectors are commonly used in motion detection applications for intrusion detection as well as for home/office automation and security systems. Fresnel lens arrays are designed so that their visibility region is divided into zones. Each lens on the array creates a cone of visibility whose size depends on the focal length of the lens and the size of the detector element. However, with a dual element pyroelectric detector, the cone is divided into two distinct zones, as illustrated in Fig. 2.5, corresponding to each of the lobes in Fig. 2.3. The response obtained when crossing one beam is exactly the opposite to that obtained crossing the other. For the sake of convenience, we designate the beam that results in a rise and then a fall in the detector response as a person enters into it as positive (+) and the other beam as negative (-). The order of occurrence of these beams depends on the path direction. The detector response observed from one lens aperture with one person walking across it is a positive and negative peak as shown in Fig. 2.6 (a). When the person moves in the opposite direction, the response is similar in nature but with opposite polarity as shown in Fig 2.6 (b). This gives the information about the direction of motion of the source assuming that the orientation of the detector is previously known.

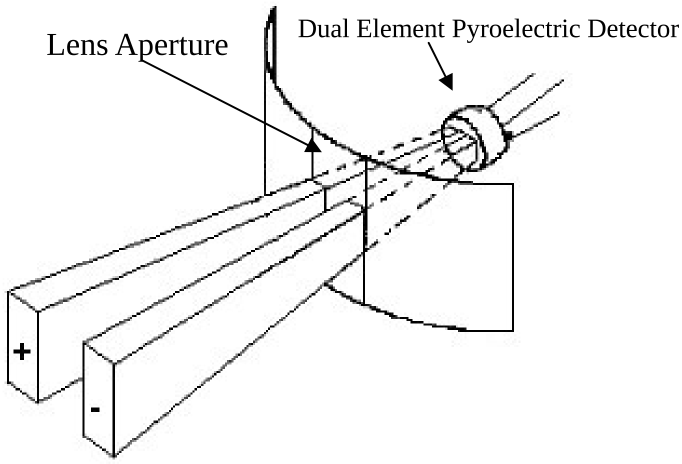

Fig. 2.5 Beams formed by a single lens on a lens array. The two beams correspond to each of the elements in a dual element detector

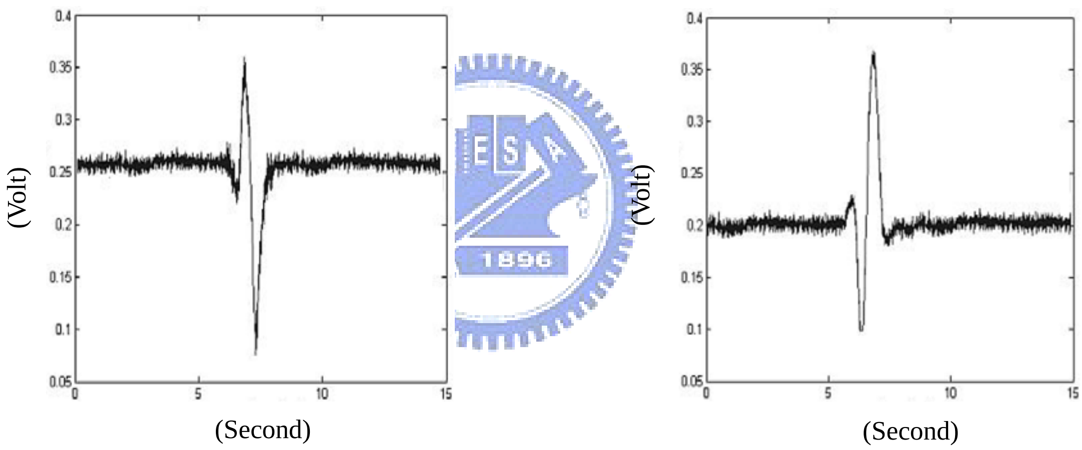

(a) (b)

Fig. 2.6 (a) Signal obtained from a dual element pyroelectric detector with a person moving across the FOV of a single lens in front of a detector. (b) Signal obtained from the detector with a person moving in the opposite direction.

We employ a commercially available lens array (Animal alley array- AA0.9GIT1) obtained from Fresnel Technologies Inc. [4]. The material of the lens has suitable transmission in the 8-14 μm. The FOV of lens array was characterized and is illustrated in Fig. 2.7. A summary of the different parameters of this lens array is shown in Table 1. Fig. 2.8 illustrates the sensor response signal, when a human target passes through the FOV of a detector with multiplex visibilities generated by a Fresnel lens array.

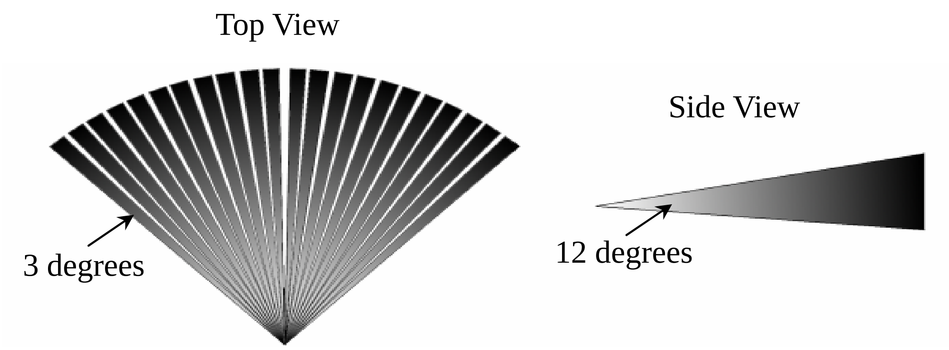

Fig. 2.7 Characteristic of FOV of Fresnal lens array. Each lens on the array creates two beams having a angular visibility of 3^{o} separated by 1^{o}.

Table 2.1 Summary of characteristics of Fresnel lens array

Parameter	Value
Angular coverage of each lens	7^{o}
Angular gap between adjacent beams	2^{o}
Angular gap between two beams from each lens	1^{o}
Lateral angular spread	12^{o}
Transmittance of lens in IR	75 %

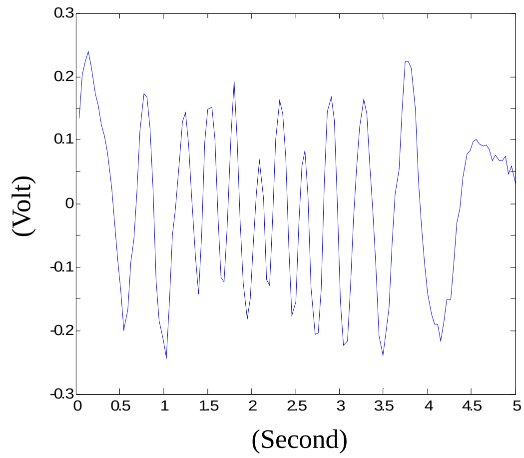

Fig. 2.8 Response signal of a dual element pyroelectric detector to a person with multiplex visibilities generated by a Fresnel lens array.

2.4 Micro-controller and Transceiver

This sensor system was implemented using the Texas Instrument micro-controller (MSP430149) and RF transceiver (TRF6901) module. The TI's MSP430149 combines computational power with a compact design and low cost. It runs on a 20MHz internal clock and contains 64K of total on-board memory, available either for programming instructions of data storage. It also features a C-language compiler for easy programming and uses memory-mapped registers that facilitate the control of an on-board 12-bit, 8 channel analog to digital converter and UART serial interface. The ADC sampling frequency can be set up to at least 150 Hz, sufficiently above the frequency required to sample a signal induced by human motion. The MSP430149 processor is augmented by a TRF6901 daughter board that controls a two-mode dual-antenna radio transmitter. The TRF6901 uses a serial port interface (SPI) to connect to the MSP430149, allowing the carrier frequency and data rate to be controlled in software. Due to the small amount of power that is coupled to the detector, the single amplitude detected from a subject is very small. In order to be able to implement signal processing, the single needs to be conditioned. We attached a custom 8-channel amplifier circuit to intervene between each detector and the analog input pins of the processor. The amplifier circuit is of standard design and has a tunable gain between 200 and 40000. Extra circuitry for adjusting the DC offset is also provided. The amplifier board can handle up to simultaneous eight channels.

2.5 Sensor Platform Construction

Each of lens holders and the support base were made using an EDEN330 rapid prototyping machine (Fig. 2.9) manufactured by Objet Geometries, Ltd. [5]. It utilized the PolyJet^{TM} Technology [5] to fabricate 3-dimensional structure. PolyJet^{TM} Technology is a layer-additive process where physical objects are built directly from a computer aided design (CAD) database. We used the CAD software Solidworks to design the 3-dimensional structure used in the sensor module. This software allows the construction of assemblies from different parts. Each of the lens holders and the support base were developed as parts and were assembled into a final unit. The description of the object CAD data is known as an STL (Stereolithography) file [6] which is then used for rapid prototyping. This file basically consists of the X, Y, Z coordinates of the three vertices of each surface triangle, as well as an index that describes the orientation of the surface normal. STL format is conceptually simple and topologically robust. With sufficient resolution, STL format can achieve high accuracy.

Fig. 2.9 The EDEN330 Rapid Prototyping device and water jet.

2.5.1 The Features of the EDEN330

PolyJet™ technology drives the precision inside the EDEN330. The features of this rapid prototyping machine are as follows [5],

Layer thickness (Z-axis): Horizontal build layers down to 16 μ.

Build size (X × Y × Z): 340mm x 330mm x 200mm.

Build resolution: X-axis: 600 dpi: 42 μ;Y-axis: 300 dpi: 84μ; Z-axis: 1600 dpi: 16 μ.

High quality: Market-leading resolution of 16μ ensures smooth, accurate and highly detailed parts and models.

Highly accurate: Precise jetting and build material properties enables fine details and thin walls (600μ or less depending on geometry and materials).

Clean: Suitable for an office environment, with non-touch resin loading/unloading, easy support removal, and easy replacement of jetting heads.

Fast: Rapid process, due to high-speed raster build at full width, simultaneous building of multiple items, and no post-curing.

Versatile: The wide variety of FullCure materials enables parts with different geometries, mechanical properties, and colors; use of the same Support material for all model types makes switching materials easy and fast.

Unattached building process: Once started the process is fully automatic and can not be attended until the process in completed.

2.5.2 Fabrication Process

PolyJet^{TM} inkjet technology works by jetting state of the art photopolymer materials in ultra-thin layers (16μ) onto a build tray layer by layer until the part is completed. Fig. 2.10 shows the brief diagram of the Object PolyJet Process [5]. As you might expect, it relies on a build platform that moves down in the Z-direction (vertical), with moving “print heads” which pass over the platform and print both the model material and the support material to build each layer. Instead of the single head in other machines, eight jetting heads simultaneously deposit identical amounts of photopolymer on the build tray with each pass along an X-axis. Once built, each photopolymer layer is then cured and hardened by exposure to UV lighting. The next layer is then built on top of that and so on. After the whole process complete, users can handle and use immediately, without any time-consuming post processing/curing. The gel-like support material, which is specially designed to support complicated geometries, is easily removed by hand and water jetting. Fig. 2.11 shows an example completed object set. After using the high-pressure water jet to wash off the supports, we obtain a finished product set, as shown in Fig. 2.12.

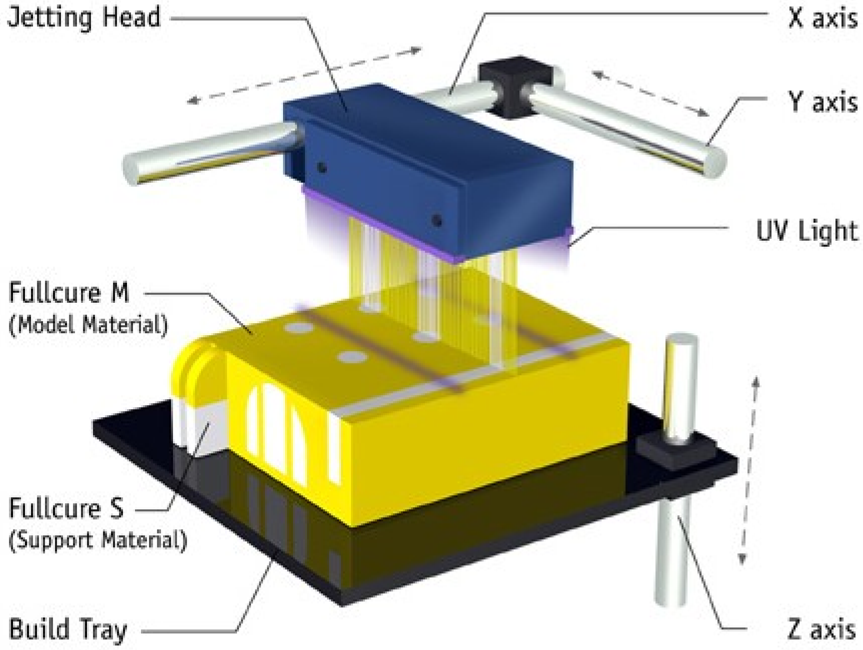

Fig. 2.10 The Object PolyJet Process.

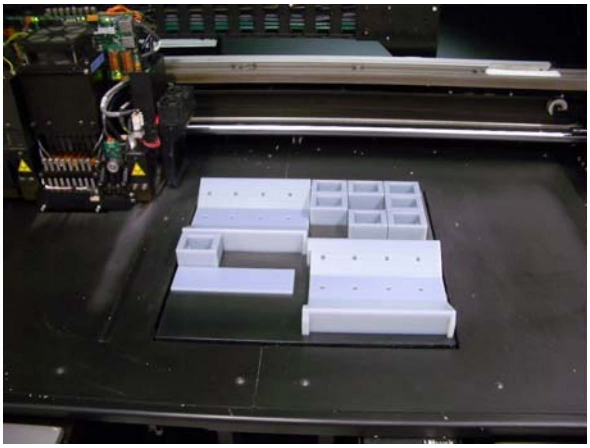

Fig. 2.11 An example completed object set.

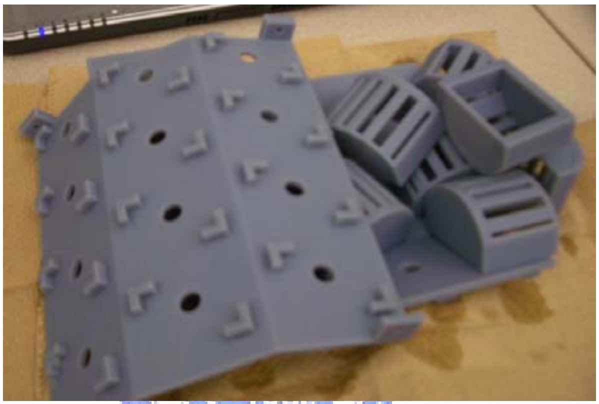

Fig. 2.12 A finished product set.

2.5.3 Fabricated Structure

In the experiments, we made two kinds of sensor modules, one for analog feature extraction and another for digital feature extraction. Fig. 2.13 shows an example sensor module for spectral feature extraction. This sensor module contains a pyroelectric detector whose visibility is modulated by a Fresnel lens array. Another kind of one-column radial type of sensor module was designed and used for walker recognition based on digital event index sequences as shown in Fig. 2.14. This sensor module has four pyroelectric detectors with the Fresnel lenses arranged in one column.

Fig. 2.13 A sensor module for spectral feature extraction.

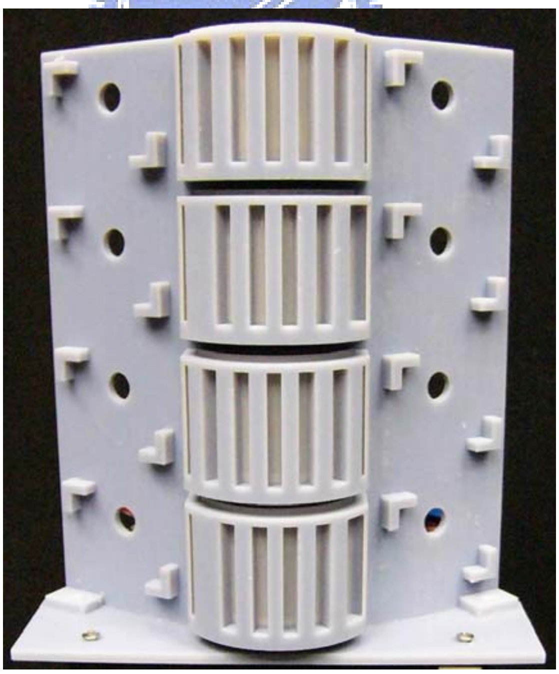

Fig. 2.14 An example sensor module contains 4 PIR detectors and with periodic sampling masks.

References for Chapter 2:

[1] Glolab Corporation, "Infrared parts manual," http://www.glolab.com/pirparts/infrared.html.

[2] Q. Hao, D. J. Brady, B. D. Guenther, J. Burchett, M. Shankar, and S. Feller, "Human tracking with wireless distributed radial pyroelectric sensors," *IEEE Sensors Journal*, 6, pp. 1683-1694 , 2006.

[3] Hengwen Optics, http://fresneloptic.com/html_en/application.htm.

[4] Fresnel Technologies Inc., http://www.fresneltech.com/arrays.html.

[5] Objet Geometries, Ltd, http://www.2objet.com.

[6] C. Hull, "Apparatus for production of three-dimensional objects by stereolithography," U.S. Patent 4,575,330, 1986.